

The anode potential regulates bacterial activity in microbial fuel cells

Peter Aelterman · Stefano Freguia · Jurg Keller ·
Willy Verstraete · Korneel Rabaey

Received: 14 November 2007 / Revised: 7 December 2007 / Accepted: 8 December 2007 / Published online: 10 January 2008
© Springer-Verlag 2007

Abstract The anode potential in microbial fuel cells controls both the theoretical energy gain for the microorganisms as the output of electrical energy. We operated three reactors fed with acetate continuously at a poised anode potential of 0 (R_0), -200 (R_{-200}) and -400 (R_{-400}) mV versus Ag/AgCl and investigated the resulting bacterial activity. The anode potential had no influence on the start-up time of the three reactors. During a 31-day period, R_{-200} produced 15% more charge compared to R_0 and R_{-400} . In addition, R_{-200} had the highest maximal power density (up to 199 W m^{-3} total anode compartment during polarization) but the three reactors evolved to the same power density at the end of the experimental period. During polarization, only the current of R_{-400} levelled off at an anode potential of -300 mV versus Ag/AgCl. The maximum respiration rate of the bacteria during batch tests was also considerably lower for R_{-400} . The specific biomass activity however, was the highest for R_{-400} ($6.93 \text{ g chemical oxygen demand g}^{-1} \text{ biomass-volatile suspended solids (VSS) d}^{-1}$ on day 14). This lowered during the course of the experiment due to an increase of the biomass concentration to an average level of $578 \pm 106 \text{ mg biomass-VSS L}^{-1}$ graphite granules for the three reactors. This research indicated that an optimal anode

potential of -200 mV versus Ag/AgCl exists, regulating the activity and growth of bacteria to sustain an enhanced current and power generation.

Keywords Biofuel cell · MFC · Electricity · Biomass yield · Respiration · Electron transfer

Introduction

The microbial activity in the anode compartment of microbial fuel cells (MFCs) is essential to liberate electrons from various organics in order to sustain the electricity generation (Allen and Bennetto 1993). The microorganisms living in the anode use the conductive electrodes to drive their energy metabolism to survive and grow in this specific environment (Chaudhuri and Lovley 2003). In order to maximise the electricity generation using MFCs, the reactor, the biocatalyst and the interaction between both need to be optimised to fully exploit the capacities of microbial fuel cells.

The anode potential is an important factor controlling this synergistic interaction as it can influence the electron liberating capacities of the biocatalyst. From a thermodynamic point of view, the anode potential determines, apart from the metabolic pathway used, the theoretical energy gain for the biocatalyst (Schroder 2007). The energy gain for the bacteria can be calculated using the following equation:

$$\Delta G^{\circ'} = -n.F.(E^{\circ'}_{\text{donor}} - E^{\circ'}_{\text{acceptor}}) \quad (1)$$

Where $\Delta G^{\circ'}$ denotes the change of Gibbs free energy at pH 7 and 25°C, n is the number of electrons involved, F the Faraday constant ($96,485 \text{ C mol}^{-1} \text{ e}^-$) and $E^{\circ'}$ represents the

P. Aelterman · W. Verstraete (✉)
Laboratory of Microbial Ecology and Technology (LabMET),
Ghent University,
Coupure Links 653,
B-9000 Ghent, Belgium
e-mail: Willy.Verstraete@UGent.be
URL: <http://labmet.UGent.be>

S. Freguia · J. Keller · K. Rabaey
Advanced Water Management Centre,
The University of Queensland,
Gehrmann Building, Research Road,
Brisbane QLD4072, Australia

biological standard potential of the electron donor and acceptor (Thauer et al. 1977). In MFCs, the electron donor is typically an organic substrate (Liu et al. 2005, Rabaey et al. 2003), although also inorganic substrates have been described (Rabaey et al. 2006). In case of acetate as organic electron donor, which has a standard biological potential of -496 mV versus Ag/AgCl (Logan et al. 2006) and the anode electrode as the electron acceptor with a potential ranging from -400 to 618 mV versus Ag/AgCl, the theoretical energy gain for the bacteria ranges from -74 to -859 kJ per mole of acetate. Thus, the lower the anode potential, the less energy per electron transferred there is available for growth and cell maintenance. A higher anode potential may enhance the growth rate of bacteria, resulting in a higher biocatalyst density, faster starting up of the electricity generation and overall, higher current generation. However, in order to maximise the electrical energy output of a MFC, for a set current the anode potential should be as low and the cathode potential as high as possible (Logan et al. 2006). This leads to a trade-off between the anode potential wanted for the end user and the biocatalyst, suggesting the existence of an optimal anode potential range satisfying both.

Up till now, the effect of the anode potential on the biocatalyst has received only limited attention. Finkelstein et al. (2006) described how the anode potential affects the colonization of the anode of a sediment MFC by mineral-reducing microorganisms. Different oxidative potentials (-58 , 103 and 618 mV versus Ag/AgCl) were applied to a set of anodes under conditions known to promote anode enrichment of acetate oxidizing/mineral reducing microorganisms. The current generation increased from about 300 μ A to about 450 μ A as the anode potential was higher. When opening the circuit, the anode potential dropped to values which were approximately 40 to 60 mV lower compared to the original poised potential, the abiotic control electrodes remained at the original potentials. However, these open circuit potentials are high compared to the theoretical anode potential of -496 mV versus Ag/AgCl which could be reached using acetate as substrate (Logan et al. 2006). Finkelstein et al. (2006) suggested that the microorganisms adapt their electron transferring system to a level just below the anode potential and that more research is needed to understand the effects of the anode potential on the biocatalyst development.

The aim of this study was to investigate the influence of the anode potential on the start-up time, maximum current generation, the respiratory activity, the biomass concentration and maximum power generation. Therefore we simultaneously operated three identical continuous MFCs during a period of 33 days at three specific poised potentials of 0 , -200 and -400 mV versus Ag/AgCl. Periodically, the respiratory activity of the biocatalyst in the

anode was monitored using a titration and off-gas analysis (TOGA) sensor and biomass concentrations were determined using phospholipid extraction. In addition, polarization curves were recorded to monitor the maximum current and power generation.

Materials and methods

Reactor setup

Three reactors were constructed from perspex frames as described previously (Aelterman et al. 2006). The anode frames were modified to contain a sample port, a gas sparging tube, a Ag/AgCl reference electrode (RE-5B, BASi, United Kingdom) two outlets and an inlet. To obtain a homogenous liquid flow through the anode compartment, a perforated tube was installed in the anode compartment inlet. Each anode compartment had a hydraulic circuit containing an individual influent tubing, outlet tubing and a recirculation loop. The cathode frames contained an inlet and outlet to which an individual cathode recirculation loop and buffer vessel (0.5 L) was connected. A cation exchange membrane (Ultrex™ CMI7000, Membranes International Inc., USA) was used between the anode and cathode of each MFC unit. The three MFCs were separated by two rubber sheets (5 mm). The anode electrodes consisted of 125 gram of pre-wetted graphite granules (111 mL) (type00514, diameter between 1.5 and 5 mm, Le Carbone, Belgium) and a graphite rod (5 mm diameter, Morgan, Belgium) to collect the electrons. The anode compartment had a headspace of 18 mL. The cathode electrodes consisted of a two carbon felts (5 and 10 mm, SGL, Germany) and a graphite rod (5 mm diameter, Morgan, Belgium) to collect the electrons. Prior to use, the granules were washed three times with water. The total empty volume of one frame was 156 mL (TAC, total anode compartment), the void volume (NAC, net anode compartment) after installing the electrode and inlet ports amounted to 60 mL.

Operational conditions and inoculation

The three MFCs were continuously operated for 33 days at a poised anode potential of 0 (R_0), -200 (R_{-200}) and -400 (R_{-400}) mV versus a Ag/AgCl reference electrode (RE-5B, BASi, United Kingdom). Only during the short initial period (14 h) at the beginning of the experiment, the poised anode potential for all reactors was -200 mV to prevent the potentiostat from delivering electrons to the anodes due to the very low initial catalytic activity. The MFCs were inoculated with the effluent of active acetate fed MFCs. The MFCs were operated at a room temperature of 19.8 ± 1.5 °C

A sterile synthetic influent containing 0.5 g L^{-1} sodium acetate prepared as previously described (Rabaey et al. 2005c) was continuously fed to the individual MFCs by a peristaltic pump (Watson Marlow, Belgium) at a flow rate of 23 mL h^{-1} . Each MFC anode had a recirculation loop with a flow rate of $2,500 \text{ mL h}^{-1}$.

The catholyte was prepared according to Park and Zeikus (2003) and consisted of $0.5 \text{ L } 100 \text{ mM } \text{K}_3\text{Fe}(\text{CN})_6$ aqueous solution in a $3 \text{ g L}^{-1} \text{KH}_2\text{PO}_4$ and a $6 \text{ g L}^{-1} \text{Na}_2\text{HPO}_4$ buffer (Merck, Belgium) which was recirculated from the buffer vessel through the cathode matrix at a flow rate of $2,500 \text{ mL h}^{-1}$. The oxidation/reduction potential of the catholyte was controlled by a periodic renewal of the catholyte solution when the solution was decolorised.

Data acquisition, electrochemical and chemical analysis

The anode potential was continuously poised using a multichannel potentiostat (VMP3, Bio-Logic, France) versus a Ag/AgCl (197 mV versus normal hydrogen electrode (NHE)) reference electrode (RE-5B, BASi, United Kingdom) and the resulting current was recorded every 30 seconds. These values were used to calculate the hourly averaged currents and total charge production. Current values were converted to equivalent g chemical oxygen demand (COD) values using a ratio of 8 g COD per mole of electrons. Polarization curves were obtained by imposing a linear potential decrease of -1 mV s^{-1} from the open circuit voltage (OCV) potential to a cell potential of 0 mV followed by a linear voltage increase of 1 mV s^{-1} of the cell potential to the original OCV by a multichannel potentiostat (VMP3, Bio-Logic, France). During the polarization, the anode and cathode potential versus Ag/AgCL and the current were recorded. The polarization curves of the reactors were measured simultaneously and in triplicate with an intermitted OCV period of 1 h.

The acetate concentration was determined by HPLC using an ion exclusion column at $65 \text{ }^\circ\text{C}$ and a refractive index detector (RID-10A) after filtering the sample with a sterile $0.22 \text{ }\mu\text{m}$ membrane filter.

TOGA

The TOGA sensor system as developed by Pratt et al. (2003) was used to determine gas production rates in the anode compartment of the reactors described above. The TOGA sensor consists of a bioreactor, where batch experiments under controlled operational conditions can be carried out and an off-gas measurement arrangement involving the use of a mass spectrometer (Omnistar, Balzers AG, Liechtenstein), and several mass flow controllers and meters to determine the transfer rates of gaseous compounds of interest through gas-phase mass balance. A full

description of the TOGA principles can be found in studies by Pratt et al. (2003) and Gapes et al. (2003). During the TOGA experiment, both the CO_2 production-rate and the current generation at the respective poised potential of the reactor were monitored on-line. The anode compartment was continuously sparged with a helium flow (100 mL min^{-1}). First, the liquid of the anode compartment was removed and the moist granules were left in open circuit for at least 10 min to remove residual CO_2 . The OCV was not negatively affected during this operation. Next, the anodes were fed with 60 mL of a 0.250 g L^{-1} Na-acetate containing M9-medium and left in OCV for an additional 10 min. After this period, the anode potential was poised at the desired potential resulting in the generation of current and CO_2 . When the current generation reached a level of 0 mA , the circuit was opened again but the CO_2 transfer rate was recorded until it had reached the level of endogenous respiration again. After this, the experiment was stopped and the anode liquid was removed for VFA analysis. The total charge (coulombs) generated during the batch test was expressed as mg CO_2 by taking the conversion of 4 mol e^- per mol of CO_2 into account. During the 3 h preceding the next experiment performed on the reactor the circuit was opened and in case of Run1B (day 19) 60 mL of an Na-acetate (0.250 mg L^{-1}) containing M9-medium was added to the anode compartment. In the case of Run2C (day 30), 60 mL of M9 medium without acetate was added in the anode compartment.

Phospholipid analysis for determining microbial biomass

The procedure used in this study to determine microbial phospholipids was a modification of that found in Findlay et al. (1989). Samples of mixed biomass-loaded graphite granules ($1.72 \pm 0.14 \text{ g}$ of dry weight graphite granules) were withdrawn in quadruplicate from the reactor on day 14, 21 and 29 after the start of the experiment. The granules were replaced by the same amount of fresh graphite granules to maintain a same electrode volume. The procedure consisted of: (a) 2 g of wet graphite granules were added into 50 mL screw-cap test tubes. Then, 7.5 mL of chloroform, 7.5 mL of methanol and 7.5 mL of deionised water were added to the samples. The extraction mixture was gently shaken for 10 min and allowed to stand up to complete phase separation. (b) To facilitate recovery of the chloroform, the aqueous (upper) phase was aspirated from the test tubes with the aid of a glass syringe and subsamples of 2 mL of the chloroform layer were transferred into 10 mL screw-cap test tubes. At this point, lipids can be stored at $-20 \text{ }^\circ\text{C}$. (c) The chloroform was removed under a stream of nitrogen, and phosphate was liberated from lipids by adding 2 mL of a potassium persulfate solution (5 g added to 100 mL of $0.36 \text{ N H}_2\text{SO}_4$) and the sealed test

tubes were heated in an oven at 105°C for 2 h. (d) 0.45 mL of the sample was transferred in a cuvette and phosphate release by persulfate digestion was determined by adding 0.1 mL of an ammonium molybdate solution (2.5% of $(\text{NH}_4)_6\text{Mo}_7\text{O}_{24}\cdot 4\text{H}_2\text{O}$ in 5.72 N H_2SO_4 allowed to stand for 10 min) and 0.45 mL of a malachite green solution (0.111% polyvinyl alcohol (MW 22,000) dissolved in water at 80°C is allowed to cool, and 0.011% malachite green oxalate salt is then added and allowed to stand for 30 min). (e) The absorbance at 610 nm was then read using a spectrophotometer (Cary50, Varian, Australia). The concentrations of phosphate were calculated by using the regression line from a standard curve obtained by digesting 10, 20, 40, 60, 80 and 150 μL of a 1 mM glycerol-phosphate solution. Glassware was washed with a 10% (v/v) HNO_3 solution, rinsed five times with tap water and two to three times with deionised water, and air-dried. Prior to use, glassware was rinsed with chloroform. The biomass concentration was calculated based on the conversion factor of 191.7 μg of biomass-C per 100 mmol of phospholipid (Findlay et al. 1989) and a conversion factor of 2 g biomass- volatile suspended solids (VSS) per g of biomass-C based on an empirical formula of sludge organisms (Porges et al. 1953).

Results

Start-up phase

The three MFCs were inoculated simultaneously. The anode potentials of R_0 , R_{-200} and R_{-400} were poised at 0, -200 and -400 mV versus Ag/AgCl respectively and from day 1 till day 2 an average current of 4.3 ± 0.4 (R_0); 1.5 ± 0.8 (R_{-200}) and 0.5 ± 0.4 (R_{-400}) mA was generated. However, in the subsequent days, the current of the three MFCs evolved to the same level of 2.6 ± 0.6 mA (Fig. 1). Polarization curves recorded on day 7 showed a maximum current generation of 18.1 ± 1.8 mA which was similar for the three reactors. R_{-400} generated a higher maximum power of 7.3 ± 0.7 mW compared to R_0 and R_{-200} (4.2 ± 0.7 and 4.6 ± 0.6 mW, respectively). At the end of day 7, a notable increase of the current of all three MFCs was noted (Fig. 1). During a period of 14 h, the average current increased from 6.5 ± 1.4 to 22.0 ± 2.0 mA. Polarization curves recorded on day 8 (Fig. 2a) showed a maximum current of 44.4 ± 3.1 ; 50.0 ± 3.2 ; 35.9 ± 0.9 mA and a maximum power of 11.1 ± 1.3 ; 15.3 ± 1.9 ; 14.4 ± 1.5 mW for R_0 , R_{-200} and R_{-400} respectively. Although the current generation of R_{-400} was lower compared to R_{-200} , the power generation of R_{-400} was high and not notably different from R_{-200} . After 8 days, all three reactors were considered as started-up.

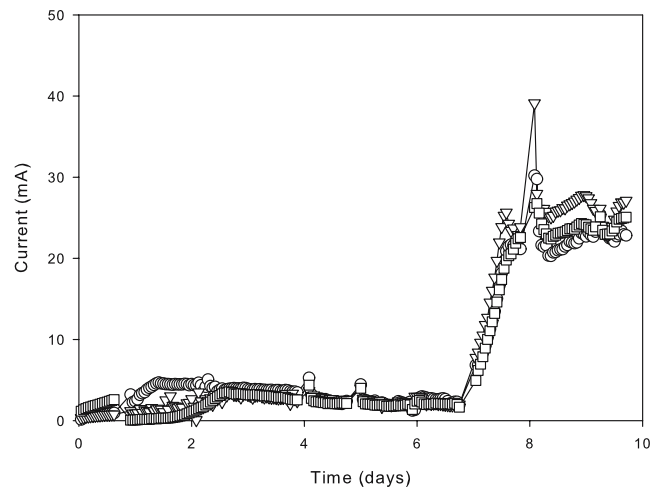


Fig. 1 Evolution of the continuous current generation (hourly averaged) during the first period after the reactors R_0 (circle), R_{-200} (triangle) and R_{-400} (square) were started

Evolution of the continuous current generation of the MFCs at three poised potentials

During the test period, both the continuous and transient currents of the three MFCs were monitored. The continuous current generation was calculated using the stable current data, excluding the transient currents. The transient currents are defined as the average current which arose during a period of 20 min after the MFCs had been in open circuit for 2 h at least. From day 8 till day 28, the stable current generation of all three MFCs remained at a constant level. R_{-200} had the highest average current generation (26.6 ± 2.2 mA) R_0 and R_{-400} generated a current of 22.3 ± 1.7 mA and 23.6 ± 1.9 mA, respectively. Based on the total coulombs produced during an operational period of 31 days, R_{-200} generated 39,535 C while R_0 and R_{-400} generated 33,473 and 33,707 C respectively. Analysis of the transient currents showed a strong increase from day 11 to day 25 (Table 1).

Evolution of the polarization curves of the MFCs operated at 0, -200 and -400 mV versus Ag/AgCl

Periodically recording polarization curves allows to monitor (a) the evolution of the maximum current and (b) power generation as well as (c) the electrochemical properties of the anode compartment. The evolution of the maximum current during polarization was similar to the evolution of the transient current production (see above). During the experimental period, R_{-200} had the highest maximum current and R_{-400} the lowest. Figure 3a shows the evolution of the maximum power. On day 25, all MFCs generated the highest power which averaged 31.1 mW or 199 W m^{-3} TAC or 517 W m^{-3} NAC. A qualitative interpretation of the

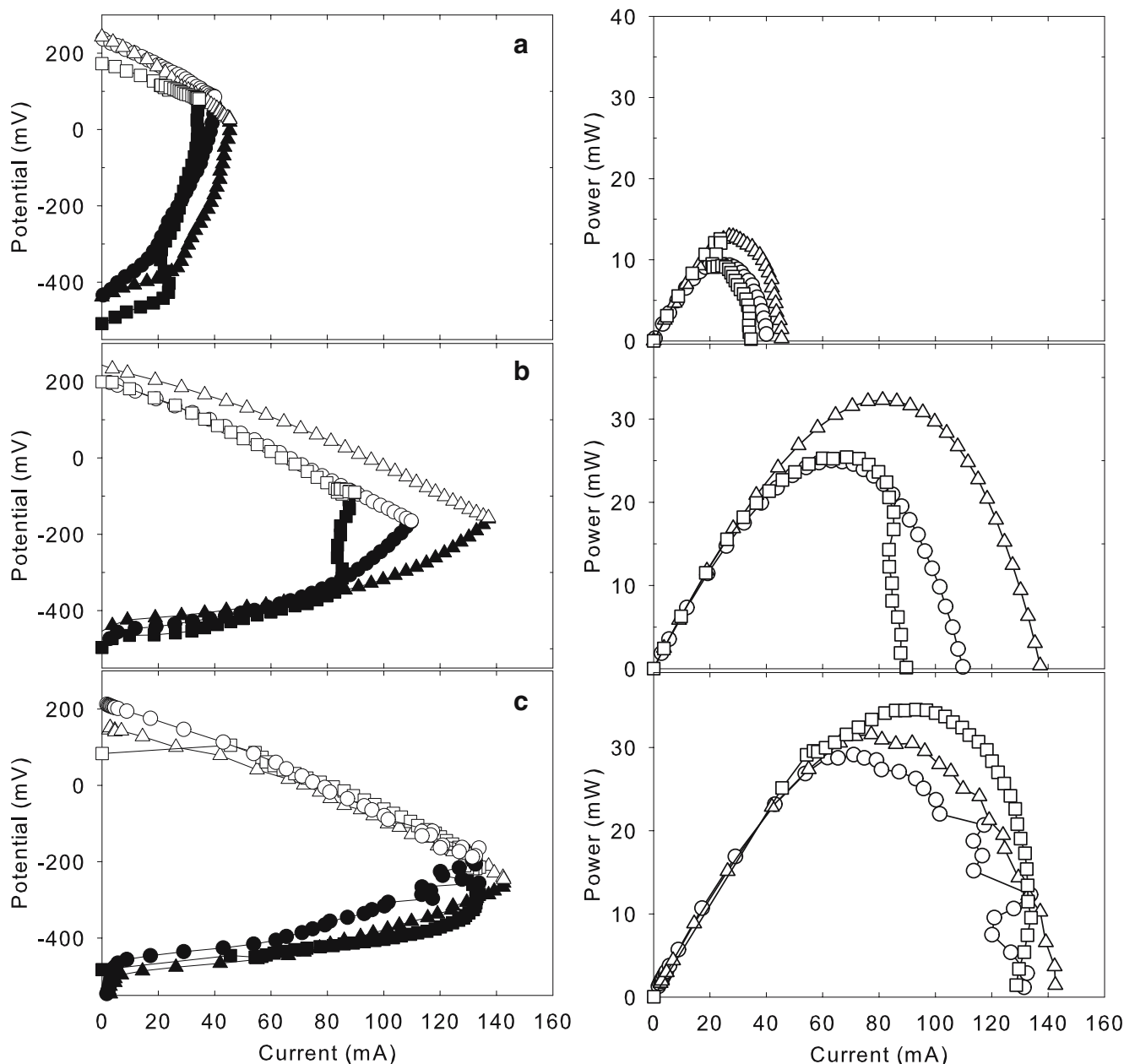


Fig. 2 The polarization curve of the anode (closed symbols) and cathode (open symbols) (left hand side) and power/current curves (right hand side) of R_0 (circle), R_{-200} (triangle) and R_{-400} (square) on days 8 (a), 17 (b) and 25 (c)

polarization curves (Fig. 2) revealed that during the whole period, the current of R_{-400} levelled off starting at an anode potential of approximately -300 mV versus Ag/AgCl. This was never observed in polarization curves of R_0 and R_{-200} . The slope of the cathodic polarization curve was similar for the three reactors and remained constant during the testing period (Fig. 2). The slope of the anodic polarization curves evolved and became less positive as the performance of the reactors increased. Figure 3b and c gives an overview of the current, cell voltage and anode and cathode potential obtained during maximum power generation. Although the cell voltage (382 ± 47 mV) at maximum power density

remained almost constant during the course of the experiment, the potential of the cathode and anode did not. The average cathode potential of the three MFCs dropped from 165 on day 3 to -104 mV versus Ag/AgCl on day 33. The average anode potential at maximum power density evolved stepwise from -202 on day 3 to -430 mV versus Ag/AgCl on day 33. From day 9 on, R_{-400} generated its maximum power at an anode potential of approximately -400 mV versus Ag/AgCl, R_{-200} and R_0 needed another 5 days to obtain this anode potential. The average current at maximum power generation of the three MFCs increased from 12 to 89 mA with a strong increase from day 7 till day

Table 1 Overview of the transient current (I_{trans} ; defined as the average current which arose during a period of 20 min after the MFCs had been in open circuit for 2 h at least), the maximum current during polarization (I_{max}) and the specific biomass activity (B_x) during the second week (days 9 (I_{trans}), 11 (I_{max}) and 14 (B_x)) and the fourth week (days 25 (I_{trans} and I_{max}) and 29 (B_x)) after inoculation

Reactor	Second week after inoculation			Fourth week after inoculation		
	I_{trans} (mA)	I_{max} (mA)	B_x (g COD g VSS ⁻¹ d ⁻¹)	I_{trans} (mA)	I_{max} (mA)	B_x (g COD g VSS ⁻¹ d ⁻¹)
R_0	29.2±2.5	44.0±1.9	3.71	165.9±37.7	167.3±10.6	2.32
R_{-200}	27.4±1.0	54.7±1.0	5.71	163.0±33.4	189.7±4.5	2.78
R_{-400}	26.4±0.7	37.4±1.3	6.93	91.9±11.8	130.3±3.8	3.20

17; overall, R_{-200} generated the highest current at its maximum power.

Bio-catalyst: quantitative evolution, activity and growth yield

The amount of bio-catalyst was monitored by means of phospholipid analysis on days 14, 21 and 29 after the start of the experiment. During this period there was a significant increase of the average biomass concentration in the three MFCs from 141.7±40.3 (day 14) to 288.5±53.0 mg biomass-C L⁻¹ granules (day 30) (Fig. 4). Although R_{-400} had, in general, a lower biomass quantity compared to R_{-200} and R_0 , this was only significant at the sample point 22 days after start up. Based on the average current generation during a 6-hour period prior to the biomass sampling expressed as equivalent g COD and the total amount of biomass in the anode compartment, the specific biomass activity could be determined (Table 1). Using the total charge generated from the start of the experiment till the first biomass sample time (current expressed as g C) and the biomass increase during this first period (wash out of biomass was not taken into account), a maximum biomass yield of 0.06 (R_0) and a minimum of 0.03 (R_{-400}) g biomass-C per g substrate-C converted in current was calculated.

Respiration rate and CO₂ production of the bio-catalyst

The respiration rate and total CO₂ production of the three MFCs during current generation at different poised potentials were quantified by the online TOGA sensor during two batch tests at different operating points (Run1 on day 19, Run2 on day 30). In the intermittent OCV period between the two batch tests, two different conditions were created: on day 19 (Run1), medium with acetate was supplied while on day 30 (Run2), medium without acetate was supplied. The total CO₂ production was compared with the total amount of coulombs generated and the amount of substrate converted which allowed to calculate several ratios (Table 2). The CO₂ production started within 2 to 3 min after the electrical circuit was closed and the average

current increased instantaneously to a value of 95.4 (R_0), 118.4 (R_{-200}) and 69.7 (R_{-400}) mA which were maintained for a period of 16, 14 and 25 min, respectively (average of Run1A and Run2A). The maximum respiration rate during

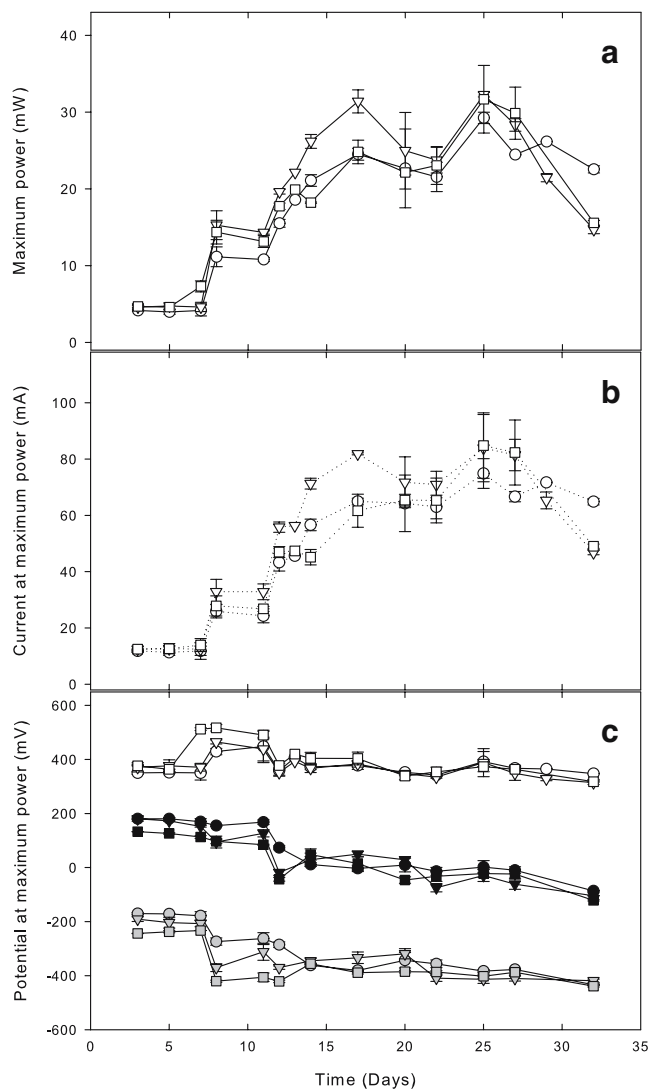


Fig. 3 Evolution of (a) the maximum power, (b) the current at maximum power and (c) cell voltage (white symbols), anode potential (grey symbols) and cathode potential (black symbols) recorded during polarization curves of R_0 (circle) R_{-200} (triangle) and R_{-400} (square) ($n=3$ for each day)

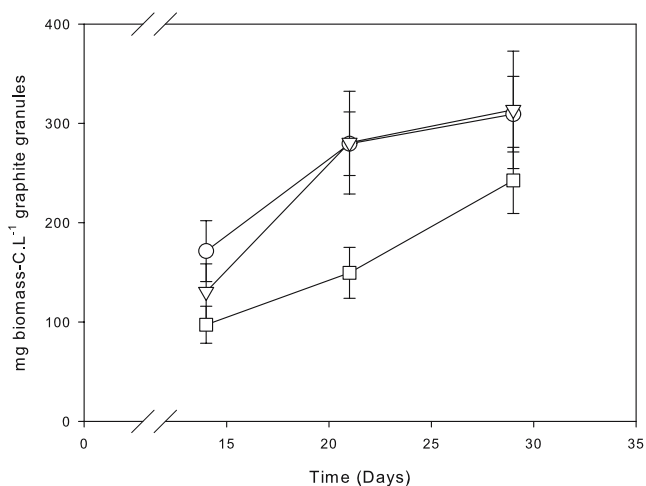


Fig. 4 Evolution of the biomass density expressed as mg biomass-C per L of graphite granules for R_0 (circle), R_{200} (triangle) and R_{400} (square) at three points in time after the start of the experiment ($n=4$)

this period was 48.0 (R_0), 61.6 (R_{200}) and 36.5 (R_{400}) mg $\text{CO}_2 \text{ h}^{-1}$ (average of Run1A and Run2A) (Table 2). After this period the current started to decline at a fast rate and eventually ceased due to a complete depletion of the medium (average 97% removal of acetate). However, even after the current production had stopped, CO_2 production continued for approximately 10 min until it reached the endogenous respiration level of approximately 5.6 mg $\text{CO}_2 \text{ h}^{-1}$. The conversion of substrate into CO_2 was close to 100% indicating a complete retrieval of CO_2 with the TOGA

(Table 2). The coulombic efficiency based on the amount of substrate consumed was between 70 and 100%. When acetate was fed during the intermittent OCV period between the batch experiments (Run1B), the charge generation was higher compared to the charge generation during Run1A. Moreover, the ratio between the current generated and total amount of CO_2 generated was around 90%, while during all the other runs, a value of approximately 80% was found. When no acetate was fed during the intermittent open circuit period (Run2C), the charge generation was lower compared to Run2A, while the substrate consumption was almost complete.

Discussion

Influence of the different poised potentials on the starting up period

The poised potential had no significant influence on the start-up time needed for the three reactors. In fact, in all three reactors, the continuous current generation quadrupled within a 12-hour period (7 days after reactor inoculation) to a level which remained fairly constant during the following 25 days. Similar observations have been made before, although the time needed for increased current generation was typically shorter, varying from 100 h (Rabaey et al. 2005b) to 50 h (Kim et al. 2005). In these cases, a five to tenfold increase of the current was observed during a period

Table 2 Overview of the maximum respiration rate, percentage of substrate consumed, the total amount of CO_2 respired and total charge generated and the ratios (after conversion to C (carbon)) of the total amount of CO_2 respired ($\text{CO}_2\text{-C-out}$), the total substrate consumed (Ac-C-used) and total charge generated (Charge-C) during the respective TOGA runs

		Max. resp. rate (mg $\text{CO}_2 \text{ hr}^{-1}$)	Acetate used ^a (%)	Total CO_2 respired (mg CO_2)	Total charge (C)	$\text{CO}_2\text{-C-out}/$ Ac-C-used	Charge-C/ Ac-C-used	Charge-C/ $\text{CO}_2\text{-C-out}$
RUN 1								
A	R_0	50.4	96	15.4	89	1.04	0.68	0.66
	R_{200}	67.5	96	14.8	101	1.00	0.78	0.78
	R_{400}	37.6	93	14.9	103	1.08	0.85	0.79
B ^b	R_0	55.6	89	14.3	116	1.03	0.95	0.92
	R_{200}	46.4	95	14.3	116	0.97	0.89	0.92
	R_{400}	29.7	94	15.3	124	1.04	0.97	0.93
RUN 2								
A	R_0	45.7	99	17.1	117	1.07	0.84	0.78
	R_{200}	55.7	94	16.4	115	1.08	0.86	0.80
	R_{400}	35.4	94	19.0	133	1.25	1.00	0.80
C ^c	R_0	32.5	98	12.8	96	0.81	0.69	0.85
	R_{200}	46.4	99	14.6	106	0.91	0.76	0.83
	R_{400}	22.0	99	15.4	108	0.96	0.77	0.80

^a Total amount CO_2 as Na-acetate supplied was 15.5 (RUN1A and B) and 16.2 (RUN2A and C) mg CO_2 .
^b During the OCV period preceding experiment B, 60 mL of a 0.25 g Na-acetate L^{-1} containing M9 medium was supplied to the anode compartment.
^c During the OCV period preceding experiment C, 60 mL of a non-carbon source containing M9 medium was supplied to the anode compartment.

of about 12 h. The factors causing this fast current increase are still unknown. As the inoculum used in this experiment was originating from a working MFC, the adaptation of the microbial community to generate electricity can be excluded as a possible reason. We hypothesise that this increase is caused by (a) the organization of the microorganisms into an effective biofilm at the electrode surface (Bond and Lovley 2003), (b) achieving a sufficient high cell density and (c) possibly the (quorum sensing regulated) onset of the production of endogenous mediating molecules or structures (Gorby et al. 2006, Rabaey et al. 2005a, Rabaey et al. 2004, Reguera et al. 2005).

Effect of the poised potential on the continuous current generation of the three MFCs

The anode potential is one of the determining elements for the energy gain for the microorganisms (Schroder 2007). The lower the anode potential, the less Gibbs free energy per electron transferred that the organisms theoretically gain. In order to increase their overall energy gain, an increase of the microbial electron transfer rate might be the result, causing an increase of the current generation. At higher anode potentials, due to the increased energy gain, the bacteria will be able to grow and reproduce faster per electron transferred. As a result, higher biomass densities can be sustained causing a potential current increase but also an increased competition for the available electrode surface and substrate. Apart from this, the enzymes, electron transferring structures and mediating molecules able to transfer electrons to the electrodes must be compliant with the electrode potential to enable an efficient electron transfer. The current generation per amount of biomass was almost double for R_{-400} compared to R_0 indicating that the biomass of R_{-400} was more active although their energy gain per electron transferred was less. During the complete testing period, the biomass concentration increased but no increase of the continuous current was noted. Moreover, only limited differences in the continuous current generation and biomass concentration existed. This could be related to the volumetric loading rate which was kept constant at a level of $1.4 \text{ g COD L}^{-1} \text{ TAC d}^{-1}$ to limit the number of variables. Based on the imposed volumetric loading rate, the maximum continuous current generation was 30 mA from which the average coulombic efficiency of 75% to 88% can be deduced. Similar MFC systems using hexacyanoferrate and mixed cultures resulted in comparable coulombic efficiencies of 75% and 78% for acetate (Aelterman et al. 2006, Rabaey et al. 2005b). The values reported here are among the highest reported in literature and indicated the highly effective microbial community relying on the electrode as single mode of respiration.

The poised potentials influenced the electricity generation at high currents

Although the loading rate determines the maximum current generation, on short term higher currents are possible after a period of open circuit operation and during polarization curves. The high current generation during the respiration experiments by R_{-400} were lower and lasted longer compared to R_0 and R_{-200} . Moreover, during the polarisation of R_{-400} , the current generation was hampered starting at an anode potential of -300 mV versus Ag/AgCl at near maximum currents (Fig. 2). This was never observed for R_0 and R_{-200} . The reason for this steep anode potential increase is not clear yet but might be caused by an enzymatic system only adapted to anode potentials lower than -300 mV versus Ag/AgCl or a lower enzymatic rate of the metabolism.

Maximum power production was dependent on the poised anode potential

After starting-up (day 7), the MFCs needed another 7 days to reach the highest power generation of 31.1 mW ($517 \text{ W m}^{-3} \text{ NAC}$ or $199 \text{ W m}^{-3} \text{ TAC}$) during polarization. This value is indicative for a well performing anodophilic microbial community and demonstrates the effective design and operation of the reactor. In general, R_{-200} performed best during the major part of the experiments both in terms of current and power generation (Fig. 3). Electrochemical analysis of bacterial strains and mixed cultures (Kim et al. 2002, Pham et al. 2008) by means of cyclic voltammetry showed that the midway redox potential of the different bacterial species had a mean value of 0 V versus NHE or -197 V versus Ag/AgCl. Moreover, the midway potential of various endogenous mediating compounds such as pyocyanine (phenazine) and 2-amino-3-carboxy-1,4-naphthoquinone (ACNQ) are around -200 mV versus Ag/AgCl (Hernandez and Newman 2001). Thus, both the electron transfer by direct cell contact and mediators have a midway potential around -200 mV versus Ag/AgCl, the potential which yielded the highest performance during this experiment.

Biomass concentrations in relation to the anode potential

Limited data about the biomass yield and biomass concentrations in MFCs exists. In accordance with the energy available for the microorganisms, a lower anode potential resulted in a lower biomass concentration. Using an average coulombic efficiency of 81%, the growth yield became 0.05 and 0.02 g biomass-C per substrate-C used. These values are lower but within the range of the biomass yields previously reported of 0 to 0.54 g biomass-C formed per g

substrate-C used (Freguia et al. 2007), 0.07 and 0.22 in glucose-fed MFCs (Rabaey et al. 2003) and comparable with the growth yield of 0.07 g biomass COD per g acetate COD used in a model presented by Picioreanu et al. (2007). The biomass density was at the maximum 0.29 g biomass-C per L of graphite granules or 0.58 g VSS per L of graphite granules which is approximately 30 times lower compared to biomass concentrations in anaerobic digesters (10–20 g VSS L⁻¹; Zinatizadeh et al. 2006). However, based on the average biomass on day 29 and the loading rate used, the specific biomass activity was 3.4 g COD g⁻¹ VSS d⁻¹ which is comparable to anaerobic systems. Biofilms growing on electrodes are subject to a duality which is rarely observed in natural conditions: the substrate concentrations are the highest at the outer layers of the biofilm while the electrode is only available at the inner layer of the biofilm. This feature requires the development of a thin and open biofilm structure which allows for a sufficient migration of substrate without hampering the transfer of electrons to the electrode. This might explain the high activity but low biomass concentrations observed in this study.

Respiration in relation to the current generation and the poised anode potential

The anode potential had an influence on the maximum respiration rate and current generation, but the coulombic efficiency was not affected. R_{-200} had generally the highest respiration rate and current generation, while R_{-400} had the lowest rate. The use of the TOGA equipment to monitor the respiration activity of MFCs online has been developed by Freguia et al. (2007). They investigated the carbon and electron balances in microbial fuel cells, which revealed the storage of substrate as polymeric material in microorganisms after a period of open circuit operation. The presence of a carbon source in the intermittent open circuit period between the two batch tests had a profound influence on the total amount of charge and CO₂ generated in relation to the amount of substrate used as shown in Table 2. The Charge-C to CO₂-C-out ratio (Table 2) was approximately 80% for most of the experiments, except when the organisms were allowed to take up substrate in a precedent period when a ratio of 90% was found. This indicates that 10–20% of the respired CO₂ is not associated with the transfer of electrons to the electrode and that these electrons are used within the microbial metabolisms or for the creation of a pool of reducing equivalents within or outside the microorganisms. Differences in total respiration and charge generation during Run1B and Run2C were related to the storage or consumption of polymeric substrate inside the cells. Moreover, the evolution of the transient currents (not shown) was proportional to the biomass concentrations

and hypothetically, the stored polymeric substrate inside the cells. Alternatively, the increased amounts of endogenous electron mediators (Rabaey et al. 2005a, Rabaey et al. 2004) and reduced sulphurous components (Rabaey et al. 2006, Straub and Schink 2004) could result in a pool of highly reduced molecules which are oxidised rapidly when the circuit is closed after a period of OCV.

Practical implications

It is complex to operate various MFCs continuously at a constant poised potential during real-life conditions as this would require the use of an expensive multichannel potentiostat. However, by monitoring the anode potential, an external resistor can be selected which enables the fuel cell to be operated at a desired range around –200 mV versus Ag/AgCl. This anode potential enabled in our test set-up the fast growth of electrochemically active biomass resulting in the highest electricity generation.

Acknowledgements This research was funded by the Research Foundation—Flanders by the FWO (project G.0172.05 and credits for a stay abroad (V4/20B-4672)). Korneel Rabaey is supported by the UQ Postdoctoral Research Fellow Scheme, the Early Career Researcher scheme and the Australian Research Council (DP0666927). The useful comments of Tom Defoirdt, Lieven Wittenbolle, Peter Clauwaert, Liesje DeSchampelaire, Gorge Ignacio and Nico Boon were highly appreciated.

References

- Aelterman P, Rabaey K, Pham HT, Boon N, Verstraete W (2006) Continuous electricity generation at high voltages and currents using stacked microbial fuel cells. *Environ Sci Technol* 40:3388–3394
- Allen RM, Bennetto HP (1993) Microbial fuel-cells—electricity production from carbohydrates. *Appl Biochem Biotechnol* 39:27–40
- Bond DR, Lovley DR (2003) Electricity production by *Geobacter sulfurreducens* attached to electrodes. *Appl Environ Microbiol* 69:1548–1555
- Chaudhuri SK, Lovley DR (2003) Electricity generation by direct oxidation of glucose in mediatorless microbial fuel cells. *Nat Biotechnol* 21:1229–1232
- Findlay RH, King GM, Watling L (1989) Efficacy of phospholipid analysis in determining microbial biomass in sediments. *Appl Environ Microbiol* 55:2888–2893
- Finkelstein DA, Tender LM, Zeikus JG (2006) Effect of electrode potential on electrode-reducing microbiota. *Environ Sci Technol* 40:6990–6995
- Freguia S, Rabaey K, Yuan ZG, Keller J (2007) Electron and carbon balances in microbial fuel cells reveal temporary bacterial storage behavior during electricity generation. *Environ Sci Technol* 41:2915–2921
- Gapes D, Pratt S, Yuan ZG, Keller J (2003) Online titrimetric and off-gas analysis for examining nitrification processes in wastewater treatment. *Water Res* 37:2678–2690
- Gorby YA, Yanina S, McLean JS, Rosso KM, Moyles D, Dohnalkova A, Beveridge TJ, Chang IS, Kim BH, Kim KS, Culley DE, Reed

- SB, Romine MF, Saffarini DA, Hill EA, Shi L, Elias DA, Kennedy DW, Pinchuk G, Watanabe K, Ishii S, Logan B, Nealson KH, Fredrickson JK (2006) Electrically conductive bacterial nanowires produced by *Shewanella oneidensis* strain MR-1 and other microorganisms. *Proc Natl Acad Sci U S A* 103:11358–11363
- Hernandez ME, Newman DK (2001) Extracellular electron transfer. *Cell Mol Life Sci* 58:1562–1571
- Kim HJ, Park HS, Hyun MS, Chang IS, Kim M, Kim BH (2002) A mediator-less microbial fuel cell using a metal reducing bacterium, *Shewanella putrefaciens*. *Enzyme Microb Technol* 30:145–152
- Kim JR, Min B, Logan BE (2005) Evaluation of procedures to acclimate a microbial fuel cell for electricity production. *Appl Microbiol Biotechnol* 68:23–30
- Liu H, Cheng SA, Logan BE (2005) Production of electricity from acetate or butyrate using a single-chamber microbial fuel cell. *Environ Sci Technol* 39:658–662
- Logan BE, Hamelers B, Rozendal R, Schröder U, Keller J, Freguia S, Aelterman P, Verstraete W, Rabaey K (2006) Microbial fuel cells: methodology and technology. *Environ Sci Technol* 40:5181–5192
- Park DH, Zeikus JG (2003) Improved fuel cell and electrode designs for producing electricity from microbial degradation. *Biotechnol Bioeng* 81:348–355
- Pham HT, Boon N, Aelterman P, Clauwaert P, De Schampelaire L, Vanhaecke L, De Maeyer K, Höfte M, Verstraete W, Rabaey K (2008) Metabolites produced by *Pseudomonas* sp. enable a Gram-positive bacterium to achieve extracellular electron transfer. *Appl Microbiol Biotechnol* 77(5):1119–29 DOI 10.1007/s00253-007-1248-6
- Picioreanu C, Head IM, Katuri KP, van Loosdrecht MCM, Scott K (2007) A computational model for biofilm-based microbial fuel cells. *Water Res* 41:2921–2940
- Porges N, Jasewicz L, Hoover SR (1953) Aerobic treatment of dairy wastes. *Appl Microbiol* 1:262–270
- Pratt S, Yuan ZG, Gapes D, Dorigo M, Zeng RJ, Keller J (2003) Development of a novel titration and off-gas analysis (TOGA) sensor for study of biological processes in wastewater treatment systems. *Biotechnol Bioeng* 81:482–495
- Rabaey K, Lissens G, Siciliano SD, Verstraete W (2003) A microbial fuel cell capable of converting glucose to electricity at high rate and efficiency. *Biotechnol Lett* 25:1531–1535
- Rabaey K, Boon N, Siciliano SD, Verhaege M, Verstraete W (2004) Biofuel cells select for microbial consortia that self-mediate electron transfer. *Appl Environ Microbiol* 70:5373–5382
- Rabaey K, Boon N, Hofte M, Verstraete W (2005a) Microbial phenazine production enhances electron transfer in biofuel cells. *Environ Sci Technol* 39:3401–3408
- Rabaey K, Clauwaert P, Aelterman P, Verstraete W (2005b) Tubular microbial fuel cells for efficient electricity generation. *Environ Sci Technol* 39:8077–8082
- Rabaey K, Ossieur W, Verhaege M, Verstraete W (2005c) Continuous microbial fuel cells convert carbohydrates to electricity. *Water Sci Technol* 52:515–523
- Rabaey K, Van de Sompel K, Maignien L, Boon N, Aelterman P, Clauwaert P, De Schampelaire L, Pham HT, Vermeulen J, Verhaege M, Lens P, Verstraete W (2006) Microbial fuel cells for sulfide removal. *Environ Sci Technol* 40:5218–5224
- Reguera G, McCarthy KD, Mehta T, Nicoll JS, Tuominen MT, Lovley DR (2005) Extracellular electron transfer via microbial nanowires. *Nature* 435:1098–1101
- Schröder U (2007) Anodic electron transfer mechanisms in microbial fuel cells and their energy efficiency. *Phys Chem Chem Phys* 9:2619–2629
- Straub KL, Schink B (2004) Ferrihydrite-dependent growth of *Sulfurospirillum deleyianum* through electron transfer via sulfur cycling. *Appl Environ Microbiol* 70:5744–5749
- Thauer RK, Jungermann K, Decker K (1977) Energy-conservation in chemotrophic anaerobic bacteria. *Bacteriol Rev* 41:100–180
- Zinatizadeh AAL, Mohamed AR, Najafpour GD, Hasnain Isa M, Nasrollahzadeh H (2006) Kinetic evaluation of palm oil mill effluent digestion in a high rate up-flow anaerobic sludge fixed film bioreactor. *Process Biochem* 41:1038–1046